The current issue and full text archive of this journal is available at
http://www.emeraldinsight.com/0961-5539.htm

Interaction between condensate film and moist air in a cross flow

Dean Besednjak and Alojz Poredoš
Faculty of Mechanical Engineering, University of Ljubljana, Ljubljana, Slovenia

Leopold Škerget
Faculty of Mechanical Engineering, University of Maribor, Maribor, Slovenia

Keywords *Turbulent flow, Condensation, Numerical analysis*

Abstract *A three-dimensional numerical analysis was carried out to study in detail the combined heat and mass transfer processes between a moist air flow and a cooled surface when film condensation occurs. A cross-flow was considered between the air flow and the film flow. A turbulent flow was modelled using the Wilcox* $k - \omega$ *turbulence model. The shape of the interface between the air and the film was treated as a moving boundary, and it was calculated with the assumptions that the interface ways remain an interface, the stress at the interface is continuous and that there is no slip at the interface. Numerical results were obtained by solving simultaneous coupled equations of the air, film and solid. The results show that the condensate film flow has a significant effect on the extended surface temperature distribution and consequently on its efficiency. It is shown that the simultaneous influence of gravity and the air flow on the condensate film results in an asymmetric velocity profile in the film as well as in the asymmetric shape of the film.*

Nomenclature

c	= moisture concentration, (kg/kg)
c_p	= specific heat, (j/kgk)
D	= diffusivity (m^2/s)
g	= gravity, (m/s^2)
H	= mean curvature of the surface, (1/m)
k	= kinetic energy, (m^2/s^2)
n	= surface unit normal vector, (−)
p	= pressure, (Pa)
Pr	= prandtl number, (−)
r	= heat of evaporation, (J/kg)
Sc	= schmidt number, (−)
T	= temperature, (K)
u	= velocity, (m/s)
x	= space coordinate, (m)

Greek letters

δ	= operator, (−)
ε	= turbulent dissipation(m^2/s^3)
μ	= dynamic viscosity, (pa s)
λ	= conductivity, (w/mk)
ρ	= density, (kg/m^3)
ω	= turbulent frequency, (1/s)
γ	= surface tension, (n/m)
σ	= surface stress, (N/m^2)

Subscripts

i, j	= coordinate
n	= normal to the surface
max	= maximum
T	= turbulent

International Journal of Numerical Methods for Heat & Fluid Flow, Vol. 12 No. 8, 2002, pp. 940-957.

DOI 10.1108/09615530210448714

Introduction

Moisture from the air will condense on a surface whenever the temperature of the surface is lower than the saturation temperature of the air moisture. Depending on the conditions of the surface it can appear in two different forms: drop condensation or film condensation. The presence of the condensate on the surface increases the heat transfer resistance, and this increase is much higher in the case of film condensation. With regard to the flow orientation between the film and the air, three different relations are possible: co-flow, counter-flow and cross-flow. The first two can be modelled using two-dimensional models, however cross-flow requires a three-dimensional approach. A simultaneous study of heat and mass transfer requires complex mathematical models. As a result, many authors who have investigated heat and mass transfer in an air flow have made the assumption that the liquid film is extremely thin. Under such conditions the transport in the film can be replaced by approximate boundary conditions for the air flow, and much of the research in this field has been limited to one-dimensional or even semi-empirical models.

Kilic and Onat (1981) used a quasilinear, one-dimensional model for vertical rectangular fins and assumed that the heat and mass transfer coefficients were constant along the fin. The efficiency of the fin and the average temperature were found to be lower in the presence of condensation than when the fin was dry.

For a fin in a laminar humid air flow, Coney *et al.* (1989) extended the model to include the influence of the condensate layer on the surface temperature distribution and efficiency. This model was also able to predict the layer thickness. They took into consideration the analogy between heat and mass transfer and assumed that the condensate film flow was only influenced by gravitational force. The flow conditions affected the film thickness, which in turn had an influence on the heat conduction resistance. Their results show that the efficiency decreases with the amount of condensation and that also depends on the flow conditions in the humid air.

For the case of low relative humidity, Kazeminejad *et al.* (1993) assumed that the thermal resistance of the condensate film is negligible because the film is much thinner than the boundary layer in a dehumidification process. Their model showed that with increasing thickness of the boundary layer the heat transfer coefficient changed as well. These changes influenced the local heat flux, the fin surface temperature and the fin efficiency.

In contrast McQuiston (1975) and Wu and Bong (1994) showed that fin efficiency was not dependent on the relative humidity of the air. Their results indicated that humidity had an influence on fin efficiency only in the case of a partially wet surface.

Chen (1991) stated in his two-dimensional analysis that stream-wise variations in the humid air's properties have a significant effect on fin performance, and that the trend is a reduction in fin efficiency. Non-uniform air properties were predicted because of the different temperature distribution along the fin base compared to that along the fin tip.

Tsay (1996) focused his attention on the interaction between the turbulent binary mixture and the condensation liquid film. He performed a detailed two-dimensional numerical analysis. The coupled two-dimensional conservation equations for the condensation liquid film and the moist air stream were solved together. The matching conditions at the liquid film/moist air interface were rigorously treated.

In our previous study (Besednjak and Poredoš, 1998) we assumed a condensate film flow to be a steady layer. The layer thickness was calculated with regard to the condensation intensity and this thickness represented an additional thermal resistance to heat transfer between the moist air flow and the cooled surface. The influence of the flow conditions on the heat and mass transfer and the temperature distribution on the cooled surface were neglected. Only the relaxation of the condensation heat was considered at the interface between the air and the film layer.

The aim of this study is to increase our understanding of the heat and mass transfer processes between a condensate liquid film and the turbulent moist air in a cross-flow (Figure 1) and to show the influence of the film flow on the temperature distribution on a cooled surface. In order to achieve this, we undertook a detailed numerical analysis. The coupled, three-dimensional energy-, moment- and continuity-conservation equations for the moist air, the condensate film and the cooled solid surface were solved together. A special effort was made to model the interface between the air and the film, the shape of which is not *a priori* known. To do this we implemented a moving boundary

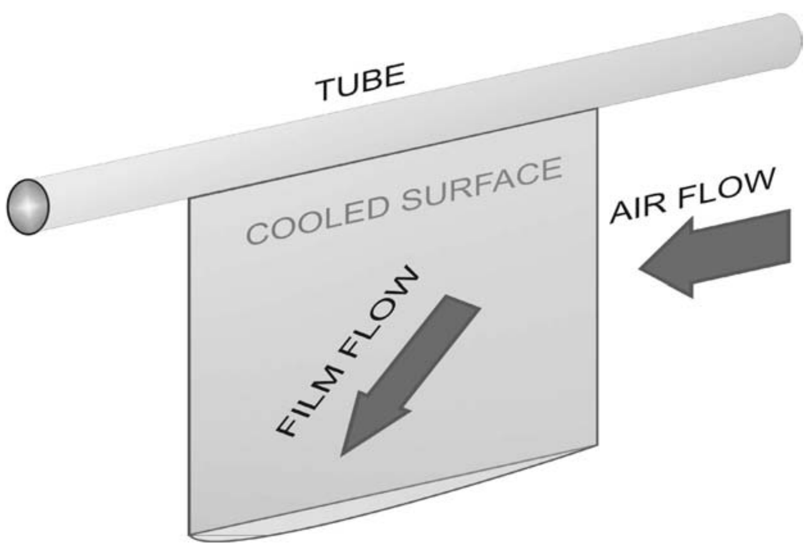

Figure 1.
Film condensation on extended cooled surface

theory. We also described the moisture phase change process on the interface very accurately.

Mathematical model

Figure 1 presents the physical system of the problem. The turbulent flow of moist air with fully developed velocity and uniform temperature is flowing over the cooled fin, which is attached to the pipe. A cooling medium in the pipe maintains a constant temperature at the fin root. As the temperature of the fin root and, consequently, also the temperature on the fin surface are lower than the dew-point temperature of the moist air, some of the water vapour condenses and forms a thin, liquid film on the fin surface. At the film-air interface, heat and mass transfer take place simultaneously. Under the influence of gravity the film tends to flow vertically down the surface. As it is also influenced by the shear force at the film-air interface, the final film flow direction is oriented diagonally downwards. This film flow regime causes a non-symmetrical film thickness geometry and requires a three-dimensional approach to problem solving.

In practical solutions for heat exchangers the air flow is mostly turbulent. Because of the low kinematic viscosity of air, laminar air flow can only be found in cases of natural convection. Classical heat transfer models include the turbulent flow and the turbulent boundary layer properties in the heat transfer coefficient. The calculation of this coefficient follows one of the known empirical models. A condensate film flow is likely to be laminar, but in the case of a lot of condensation and a higher fin, it could also be turbulent.

The simulation of heat and mass transfer in the case of air moisture condensation presents a complex problem: a set of differential conservation equations have to be solved for the air flow, the condensate film and the fin. The model of the whole problem also includes the film's moving boundary, which is influenced by an interaction between the air flow and the condensate film flow.

Basic equations for moist air

The moist air flow is treated as a steady turbulent convection flow. By considering mass conservation and Reynolds' time averaging (Wilcox, 1993), the following equations were obtained.

Continuity equation:

$$\frac{\partial u_{\mathrm{air},i}}{\partial x_i} = 0. \tag{1}$$

As the moist air is a gas mixture of dry air and water vapour, the concentration equation for water vapour was written:

$$\rho_{\text{air}}\left(u_{\text{air},j}\frac{\partial c_{\text{moisture}}}{\partial x_j}\right)=\frac{\partial}{\partial x_j}\left(\rho_{\text{air}}(D_{\text{moisture}}+D_{T,\text{moisture}})\frac{\partial c_{\text{moisture}}}{\partial x_j}\right). \tag{2}$$

$D_{T,\text{moisture}}$ represents the transport of moisture due to fluctuating turbulent motion. This is known as turbulent diffusivity and can be calculated from:

$$D_{T,\text{moisture}}=\frac{\mu_{T,\,\text{air}}}{\rho_{\text{moisture}}\cdot \mathrm{Sc}_{T,\text{moisture}}}, \tag{3}$$

where Sc_T is the turbulent Schmidt number, which depends on the turbulent nature of the flow and hence is a function of position. This is in contrast to *Sc*, the Schmidt number, which depends on fluid properties. The local value of Sc_T could be calculated using empirical models [7], but in most simulations of turbulent flow a value close to unity is suggested[7]. For our case the recommended value is 0.9 (Wilcox, 1993).

Momentum conservation equation:

$$\rho_{\text{air}}u_{\text{air},j}\frac{\partial u_{\text{air},i}}{\partial x_j}=-\frac{\partial p_{\text{air}}}{\partial x_i}+\frac{\partial}{\partial x_j}\left((\mu_{\text{air}}+\mu_{T,\text{air}})\left(\frac{\partial u_{\text{air},i}}{\partial x_j}+\frac{\partial u_{\text{air},j}}{\partial x_i}\right)-\frac{2}{3}\delta_{ij}\right), \tag{4}$$

where $\mu_{T,\text{air}}$ is a turbulent or molar viscosity. The turbulent viscosity can be expressed with the turbulent kinetic energy k and the dissipation of the turbulent kinetic energy ε. The latter transforms kinetic energy into heat. To calculate $\mu_{T,\text{air}}$ one of the turbulence models is used.

K$-\omega$ *turbulence model*. In the case of the simulated turbulent flow of humid air with a dominant boundary layer influence and the condensate film flow, the Wilcox ($k-\omega$) turbulence model is used (Wilcox, 1993). The turbulence frequency ω is connected to the turbulent kinetic energy k and the turbulent dissipation ε through the simple relation $\varepsilon=\omega\kappa$. Thus, the turbulent viscosity is calculated from the equation:

$$\mu_T=c_\mu\cdot\rho\cdot\frac{k}{\omega}, \tag{5}$$

with k and ω obtained from the following Wilcox's model transport equations (Wilcox, 1993):

$$\rho\frac{\partial k}{\partial \tau}+\rho u_j\frac{\partial k}{\partial x_j}=\frac{\partial}{\partial x_j}\left[\left(\mu+\frac{\mu_T}{\sigma_k}\right)\frac{\partial k}{\partial x_j}\right]+G-\rho\omega k, \tag{6}$$

$$\rho\frac{\partial \omega}{\partial \tau}+\rho u_j\frac{\partial \omega}{\partial x_j}=\frac{\partial}{\partial x_j}\left[\left(\mu+\frac{\mu_T}{\sigma_\omega}\right)\frac{\partial \omega}{\partial x_j}\right]+c_1\frac{\omega}{k}G-c_2\rho\omega^2, \tag{7}$$

where c_μ,c_1,c_2 are Wilcox's turbulence model constants, σ_k is a turbulent kinetic energy diffusion constant, and σ_w is a turbulence frequency diffusion constant. The values of the mentioned constants are shown in Table I. The variable G is the generation rate of the turbulence:

$$G = \mu_T \left(\frac{\partial u_i}{\partial x_j} + \frac{\partial u_j}{\partial x_i} \right) \frac{\partial u_i}{\partial x_j}. \tag{8}$$

An advantage of using this turbulence model is that we have the possibility to predict the influences of a turbulence field in the near-wall region, e.g. the moist air flow boundary layer close to the water layer, without the need to use special wall functions. Together with a fine near-wall mesh, the model provides us with a solution for the mean flow variables and the turbulence variables in the main air flow and the boundary layer as in the condensate film flow.

Energy equation. The heat transfer in the main turbulent flow is mostly convective and depends on the flow velocity field. In the boundary layer the convection is substituted by molecular diffusion, and the heat transfer intensity is reduced. The heat transfer in the main flow is calculated using a differential equation of energy conservation (Wilcox, 1993):

$$\rho_{\mathrm{air}} c_{p,\mathrm{air}} \left(u_{\mathrm{air},j} \frac{\partial T_{\mathrm{air}}}{\partial x_j} \right) = \frac{\partial}{\partial x_j} \left((\lambda_{\mathrm{air}} + \lambda_{T,\mathrm{air}}) \frac{\partial T_{\mathrm{air}}}{\partial x_j} \right), \tag{9}$$

where $\lambda_{T,\mathrm{air}}$ is a turbulent conductivity and is calculated from:

$$\lambda_{T,\mathrm{air}} = \frac{c_{p,\mathrm{air}} \mu_{T,\mathrm{air}}}{\mathrm{Pr}_{T,\mathrm{air}}}, \tag{10}$$

where $\mathrm{Pr}_{T,\mathrm{air}}$ is the turbulent Prandtl number. Its value is suggested[7] to be, in general, close to unity. Considering the flow conditions and the flow geometry, in our case its recommended value is 0.9 (Wilcox, 1993).

Boundary and interface conditions. To solve the air momentum equations the inlet velocity and velocity at the channel wall have to be defined. At the channel wall the no-slip conditions for all three components of the velocities is assumed. The boundary conditions for the air energy equation are prescribed in a similar way. The air inlet temperature is known, as is the heat flux at the channel wall, which is zero because it is treated as an adiabatic wall. The water vapour concentration at the inlet is also defined.

c_1	c_2	c_μ	σ_k	σ_ω
0.555	0.8333	0.09	2	2

Table I. Wilcox's turbulence model constants

Basic equations for the condensate film

The condensate film flow is assumed to be a laminar flow. The steady laminar momentum and the heat transfer in the film can then be described by the following equations:

Momentum equation:

$$\rho_{\text{film}} u_{\text{film},j} \frac{\partial u_{\text{film},i}}{\partial x_j} = -\frac{\partial p_{\text{film}}}{\partial x_i} + \frac{\partial}{\partial x_j}\left(\mu_{\text{film}}\left(\frac{\partial u_{\text{film},i}}{\partial x_j} + \frac{\partial u_{\text{film},j}}{\partial x_i}\right)\right) + \rho_{\text{film}} g. \quad (11)$$

The last term in equation (11) represents the gravity volume force acting on the film. It has a significant effect on the film flow compared to the air flow due to the water density, which is 10^3 times higher than the air density.

Energy equation:

$$\rho_{\text{film}} c_{p,\,\text{film}} \left(u_{\text{film,j}} \frac{\partial T_{\text{film}}}{\partial x_j}\right) = \frac{\partial}{\partial x_j}\left(\lambda_{\text{film}} \frac{\partial T_{\text{film}}}{\partial x_j}\right).$$

Boundary and interface conditions. The condensate film layer is located between the air flow and the fin. Thus to solve the film a system of equations for the film, the interface conditions on the contact face have to be defined.

Between the film and the fin the continuity of the temperature and the heat flux:

$$T_{\text{film},i} = T_{\text{fin},i}, \quad (13)$$

$$\lambda_{\text{film}} \frac{\partial T_{\text{film}}}{\partial x_j} = \lambda_{\text{fin}} \frac{\partial T_{\text{fin}}}{\partial x_j} n_j, \quad (14)$$

as no-slip conditions are required

$$u_{\text{film},j} = u_{\text{fin},j} = u_{\text{film-fin},j} = 0. \quad (15)$$

The interface conditions between the film and the air are far more complicated. The temperature at the interface is continuous.

$$T_{\text{film},i} = T_{\text{air},i} \quad (16)$$

The temperature of the film surface, which is lower than the moisture dew-temperature, ensures the conditions for a continuous moisture condensation from the air flow. This moisture flow represents a mass source for the film. The velocity of the moisture condensation, on the other hand, represents a velocity boundary condition in a direction normal to the surface.

$$u_{\text{film},n} = u_{\text{moisture},n}\frac{\rho_{\text{moisture}}}{\rho_{\text{film}}} = -\left(\left(\frac{D+D_T}{1-c}\right)\frac{\partial c}{\partial x_n}\right)\frac{\rho_{\text{moisture}}}{\rho_{\text{film}}}. \tag{17}$$

Energy balance at the interface:

$$-\lambda_{\text{film}}\frac{\partial T_{\text{film}}}{\partial x_j}n_j = -(\lambda_{\text{air}}+\lambda_{\text{air},T})\frac{\partial T_{\text{air}}}{\partial x_j}n_j + u_{\text{moisture},j}\rho_{\text{moisture}}\, r\, n_j. \tag{18}$$

The heat flux entering the film from the air also contains a latent heat flux released during the condensation of the air mixture.

The added water mass flow to the film means that the geometry of the film is not *a priori* known. Consequently, the film thickness is calculated simultaneously with the other unknown physical quantities. With the help of the moving boundary theory some additional interface conditions are defined to enable us to calculate the film geometry.

Kinematic conditions require that the interface always remains an interface:

$$(u_j n_j)_{\text{film}} = (u_j n_j)_{\text{air}} = 0. \tag{19}$$

The stress at the interface is continuous:

$$\sigma_{\text{film},i} - \sigma_{\text{air},i} = 2\gamma H n_i, \tag{20}$$

where H is the mean curvature of the surface and γ is the surface tension.

An additional no-slip condition at the interface is required:

$$n_j(u_{\text{film},t} - u_{\text{air},t}) = 0 \tag{21}$$

where u_t is the tangential velocity at the interface.

Basic equations for a solid extended surface

Heat transfer in the fin is treated as steady conduction in solids. As the fin is a solid, only the energy equation is solved.

$$\frac{\partial}{\partial x_j}\left(\lambda\frac{\partial T_{\text{fin}}}{\partial x_j}\right) = 0. \tag{22}$$

Boundary and interface conditions. The solid energy equation can only be solved if the boundary and interface conditions are known. The energy equation boundary conditions are temperature or heat flux. In our case, the temperature boundary condition is the temperature at the fin root

$$T_{\text{fin}} = T_{\text{fin,root}}. \tag{23}$$

The interface conditions at the contact face between the film and the fin have to be provided. The temperature continuity:

$$T_{\mathrm{film},i} = T_{\mathrm{fin},i}, \tag{24}$$

and continuity of heat flux are required.

$$\lambda_{\mathrm{film}} \frac{\partial T_{\mathrm{film}}}{\partial x_j} = \lambda_{\mathrm{fin}} \frac{\partial T_{\mathrm{fin}}}{\partial x_j} n_j. \tag{25}$$

Numerical modelling

The system of differential equations that describe the problem of heat and mass transfer during the film condensation of air moisture on a cooled vertical surface was solved by the finite element method (FEM). Software called Fluid Dynamic Analyses Package (FIDAP) was used for this purpose.

An adequate description of the problem is geometry (Figure 1) which was made to fulfill the needs of the simulation. In defining the geometry, we considered that the cooled surface is installed in a horizontal channel and that the problem is axis-symmetrical with regard to the channel's longitudinal axis. The geometry of the problem was divided into three control volumes (Figure 2). The air, the film and the cooled surface were the three sub-areas corresponding to the defined control volumes. Each of these sub-areas was characterized by unique physical characteristics and flow conditions.

The control volume is *cooled surface* (Figure 2) which represents the cooled vertical fin attached to the pipe. Its dimensions are $100 \times 100 \times 0.3$ mm. The fin is made of copper and attached to the bottom side of a copper pipe in which a cooling medium is flowing. The temperature of the cooling medium indirectly defines the temperature boundary condition at the fin root.

The film (Figure 2) represents a water film, which formed as a result of air moisture condensation, and flows off the fin under the influences of gravity and air flow. The film has the thermophysical properties of water. The shape of the film's control volume was based on the assumption that the cooled surface was fully wetted. Although the film thickness was not *a priori* known the FIDAP software was able to estimate it. Based on this information we chose, the thinnest possible film that still made meshing possible. The choice was conditioned by FIDAP, which prescribes the minimum dimension of a finite element. The minimum film thickness that we could use was 0.01 mm (Figure 3). The prismatic shape of the control volume also has a physical background. It considers that the film thickness at the fin root is zero, and then it slightly increases downwards. A similar situation occurs at the front fin edge, where the film thickness is also zero, and then it increases along the fin in the direction of the air flow.

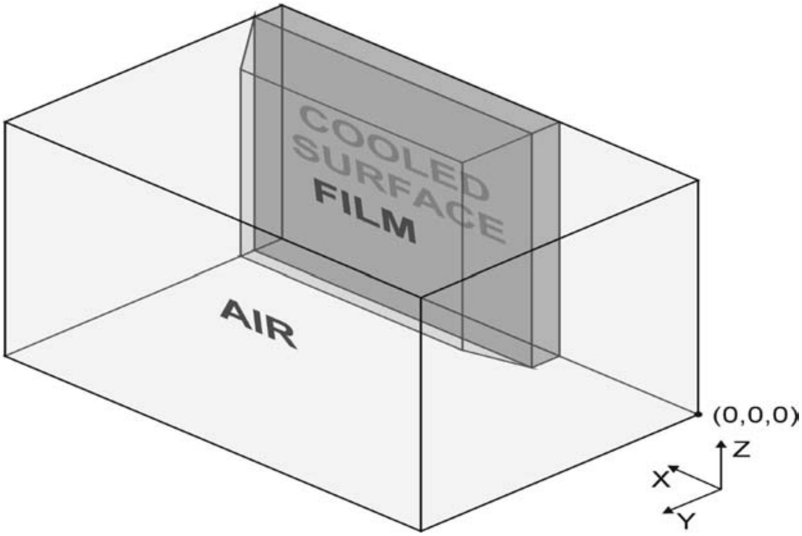

Figure 2.

The air control volume (Figure 2) represents the moist air flow. This control volume also inherits an additional so-called inlet-air flow zone that is a part of the control volume that is needed to facilitate the simulation of the correct inlet and boundary air flow conditions.

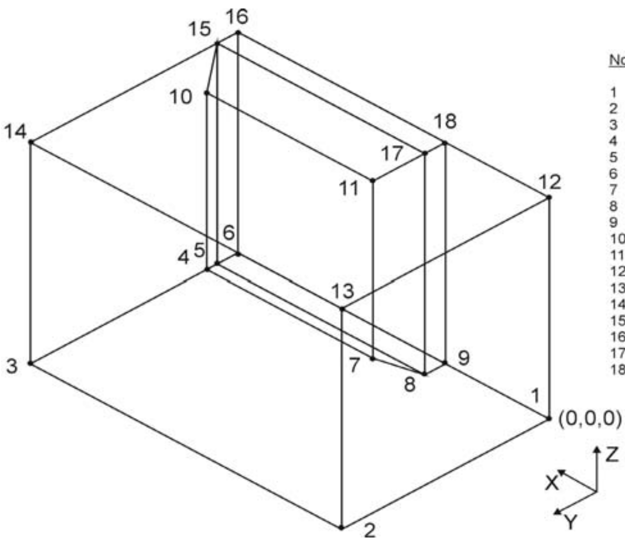

Node coordinates [mm]:

	x	y	z
1	0	0	0
2	0	90	0
3	150	90	0
4	150	0.31	0
5	150	0.3	0
6	150	0	0
7	55	0.31	0
8	50	0.3	0
9	50	0	0
10	150	0.31	95
11	55	0.31	95
12	0	0	100
13	0	90	100
14	150	90	100
15	150	0.3	100
16	150	0	100
17	50	0.3	100
18	50	0	100

Figure 3.
Control volume node coordinates

Finite elements mesh
Using a mesh generator the air, film and cooled surface control volumes were meshed. The local mesh density was chosen with regard to the expected intensity of the changes to the physical quantities. The study of the moisture phase-change phenomenon at the interface between the air flow and the condensate film requires a finer mesh in this region. Also, in the case of a dry surface a refinement of the mesh close to the interface between the air and the fin is required. Because of the three dimensional nature of the problem we used three-, two- and one-dimensional finite elements. The number of elements used to mesh the control volumes and their adequate density had a significant influence on the final result of the numerical modelling. However, with an appropriate refinement of the mesh its influence on the final results were eliminated. The final mesh contained 47,249 finite elements. The number of elements and the number of equations in the model had a direct influence on the solution time.

Simulation
FIDAP, already contains several routines to solve problems relating to heat and mass transfer. Due to the requirements incorporated in our mathematical model, some modifications to the FIDAP program code were made. We programmed additional routines to first calculate the moisture concentration boundary condition and then to calculate the intensity of the moisture condensation and the released air moisture condensation heat flux at the interface between the film and the air.

A simulation was done considering the following assumptions:

(1) the process under consideration was treated as a stationary one,
(2) the fin material is homogeneous and isotropic so its heat conduction is constant and independent of the local coordinates and temperature;
(3) the thermal conductivity and the density of the air were constant;
(4) the diffusivity of the water vapour in the air was constant;
(5) the temperature of the fin root was constant;
(6) the air flow was a fully developed turbulent flow;
(7) Gravity only influenced the film flow;
(8) there was no slip at the interface between the film flow and the fin;
(9) there was no slip and stress was continuous at the interface between the film flow and the air flow;
(10) the film's free surface was continuous.

The large number of equations used in the mathematical model to describe the condensation of the air moisture on a vertical surface is an indication of the complexity of the problem under consideration. As simultaneous solving of all the equations leads to a diverging solution, the equation-solving was performed in a cyclic three-step procedure.

In the first step, the velocity of the air was calculated using equation (4), considering the film as a steady layer. At this stage, the equations for air energy (equation 9) and concentration (equation 2) were not involved in the calculation. After calculating the air velocity field we used it as an initial condition for the calculation of the temperature and concentration distribution in the air.

The film's moment equations were included in the second step. The known distributions of temperature, velocity and concentration in the air were used as the initial conditions in this step. Only in this way, the calculation of the interface condition of the air moisture condensing velocity (equation 17) was possible. In this step the moving film was considered, but it was assumed that its thickness did not change. The latter assumption was necessary for us to calculate the initial film flow velocity profile for the next step.

In the third step, using the values calculated in the previous step, as initial velocities of the air and the film, we calculated the film thickness. The final position of the film's free surface was calculated step-by-step after considering the required interface conditions using equations (19-21). This means that first we had to calculate the air and the film velocities until they started to converge. Once the velocity solution had satisfied the convergence criteria we could start calculating the film thickness and readjust the mesh in the interface zone. This procedure was repeated until the film thickness reached its convergence criteria too. The involvement of the surface tension of the condensate film in the mathematical model meant including an additional non-linearity that causes an unstable solution. For this reason we included the surface tension value in the calculation step-by-step: from its initial value of zero to its final value. This meant we had to repeat the third step of the calculation several times.

So the final free-surface shape of the film is a result of the net condensate flow across the film boundaries and velocity-stress conditions at the interface between the film and the air.

Results of the numerical modelling

A simulation was performed for a stationary case of heat and mass transfer on a cooled extended surface (Figure 2) with the parameters shown in Table II. The results of the simulation are the velocity and temperature fields of the air flow, film flow and extended surface, as well as the shape and thickness of the condensate film layer.

As the air flow is fully developed in the inlet region, the solid cooled surface splits into two parts. An analysis of the air flow velocity profile provides good feedback information about the air flow conditions. The velocity profile of the u_z component in Figure 4 shows that an interaction exists between the air flow and the film flow; the u_x velocity component of the air flow is induced by the condensate film flow; at the same time the air flow induces the u_y velocity component in the film flow (Figure 5). The change of the u_z profile along the z axis shows that the influence of the interaction increases downward and along the cooled surface. However, this influence on the air flow could be neglected because u_z is thousand times smaller than the u_x *or* u_y velocity components. In Figure 5 the velocity vectors of the film flow are directed diagonally downward, and not vertically downwards as in the case of Nusselt condensation theory (Stephan, 1992).

As a consequence the film shape also changes and follows the film velocity (Figure 6). The film thickness is no longer constant it remains fixed along the fin as assumed (Besednjak and Poredoš, 1998), but becomes thicker in the direction of the condensate flow. Thus the thickest part of the condensate film layer is found at the bottom and at the back edge of the extended cooled surface.

The interaction between the air and the fin also influences the heat and mass transfer. Figure 7 shows that the temperature distribution on the cooled, extended solid surface follows the condensate film's velocity profile. Due to the direction of the film flow, the film becomes thicker at the bottom left corner, which has an effect on the heat transfer and the fin's surface temperature. The lower temperature in this region compared to the temperature at the right-hand bottom corner has two possible causes. First, the thicker film in this region increases the resistance to heat transfer between the air flow and the fin. Second, the higher velocity in that region increases the convective heat transfer in the film, which is flowing from the colder to the warmer part of the surface, and consequently the temperature of solid, extended surface decreases direction of the film flow.

The influence of condensate film on heat transfer

During the process of moisture condensation not only does a phase change occur but also additional condensation heat is released. The temperature field, which is formed on the extended surface also depends on the type of condensation. In the case of film condensation, a thin, continuously moving

Table II. Cooled fin and air inlet parameters

A cooled fin		Inlet air	
Material	Cu	Temperature	50°C
Root temperature	30°C	Relative humidity	50%
		Velocity	1 m/s

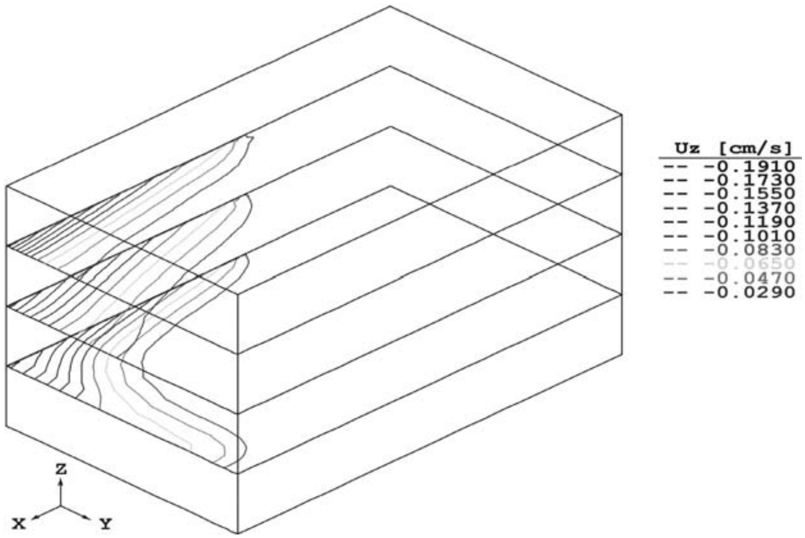

Figure 4.
Component u_z of air flow velocity field $u_{air,in} = 1\,m/s$, $t_{air,in} = 50°C$, $\varphi_{air,in} = 50\%$, $t_{root} = 2°C$

water layer exists between the extended surface and the moist air flow, and this influences the conditions of heat transfer. On the other hand, there is no layer in the case of drop condensation, where only condensate drops appear on the surface.

We performed a comparative simulation for different types of condensation forming on the extended surface. Using the same problem geometry (Figure 2),

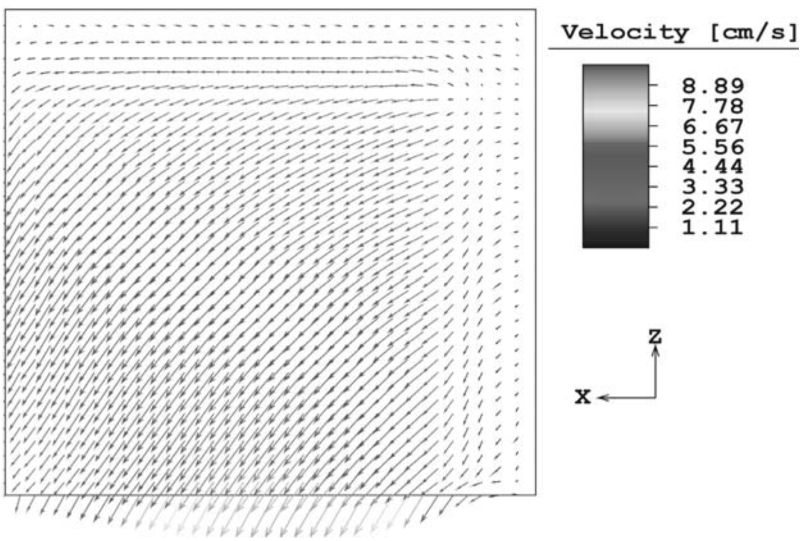

Figure 5.
Velocity distribution on a condensate film free surface, $u_{air,in} = 1\,m/s$, $t_{air,in} = 50°C$, $\varphi_{air,in} = 50\%$, $t_{root} = 2°C$

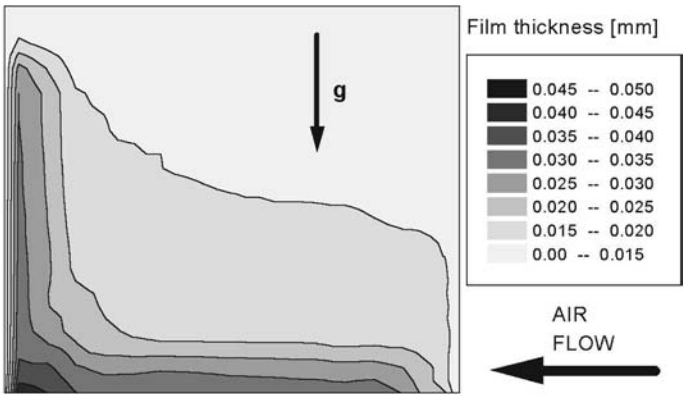

Figure 6.
Condensate film thickness, $u_{\mathrm{air,in}} = 1\,\mathrm{m/s}$, $t_{\mathrm{air,in}} = 50°\mathrm{C}$, $\varphi_{\mathrm{air,in}} = 50\%$, $t_{\mathrm{root}} = 2°\mathrm{C}$

the same boundary conditions and the same physical properties as already defined, we looked at three different cases:

(1) no condensation: dry surface;

(2) film condensation: steady film;

(3) film condensation: moving film.

These simulations were performed to show the influence of a moving film on the fin's surface temperature and heat transfer. In the literature, different approaches of heat transfer in the case of moisture condensation from air can be found. For instance, Kazminejad *et al.* (1993) and Chen (1991), analysing the heat transfer between moist air and a cooled surface, only considered the additional heat flux released due to condensation, while at the same time they neglected the influence of the condensate film.

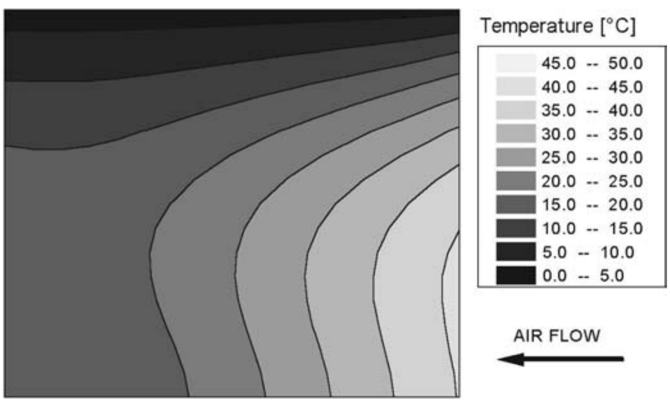

Figure 7.
Temperature distribution on a cooled surface in the case of film condensation – moving film, $u_{\mathrm{air,in}} = 1\,\mathrm{m/s}$, $t_{\mathrm{air,in}} = 50°\mathrm{C}$, $\varphi_{\mathrm{air,in}} = 50\%$, $t_{\mathrm{root}} = 2°\mathrm{C}$

In Figures 7-9 the simulated temperature fields of the cooled, extended surface are presented. In the case when the cooled air is dry or the moisture content is low and condensation does not occur, a temperature profile as shown in Figure 8 is formed. As the temperature gradient is smaller than in the case with condensation the transferred heat flux is also smaller (Figure 10). The transferred heat flux in this case is 53 per cent lower than in the case of moving film condensation (Figure 7). The higher transferred heat flux is also the reason why the presence of condensation is more desirable.

In Figures 7 and 9 the temperature profiles on the extended surface in the case of film condensation are shown. In the first case (Figure 7) a moving condensate film flow is considered, while in the second case the condensate film is steady and treated as a solid, water layer. The difference between the two cases is clearly seen in different temperature distributions on the cooled surface. The temperature gradient, the mean surface temperature and the transferred heat flux are higher in the case of the steady, water film.

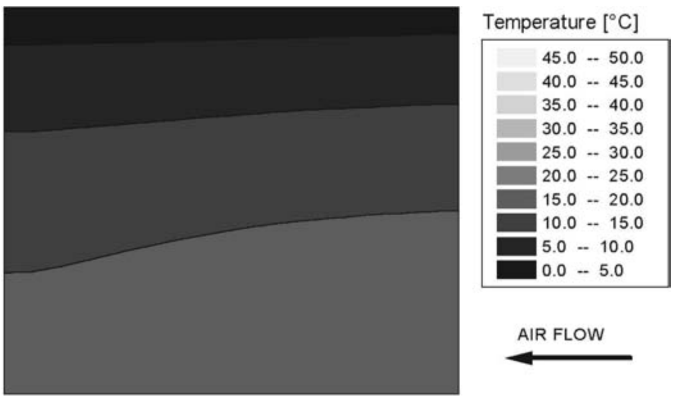

Figure 8. Temperature distribution on a cooled dry surface, $u_{\mathrm{air,in}} = 1\,\mathrm{m/s}$, $t_{\mathrm{air,in}} = 50°\mathrm{C}$, $\varphi_{\mathrm{air,in}} = 0\%$, $t_{\mathrm{root}} = 2°\mathrm{C}$

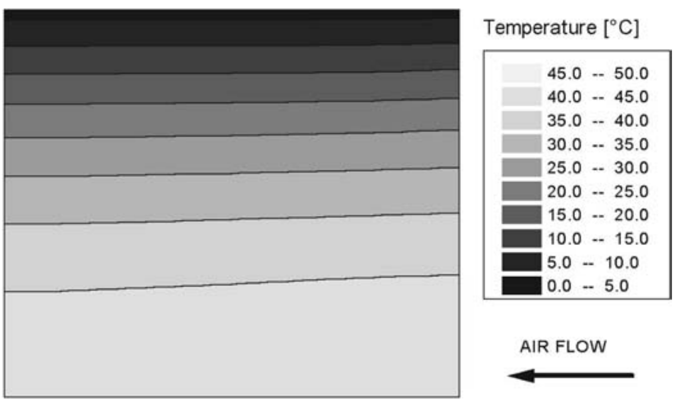

Figure 9. Temperature distribution on a cooled surface in a case of film condensation – steady film, $u_{\mathrm{air,in}} = 1\,\mathrm{m/s}$, $t_{\mathrm{air,in}} = 50°\mathrm{C}$, $\varphi_{\mathrm{air,in}} = 50\%$, $t_{\mathrm{root}} = 2°\mathrm{C}$

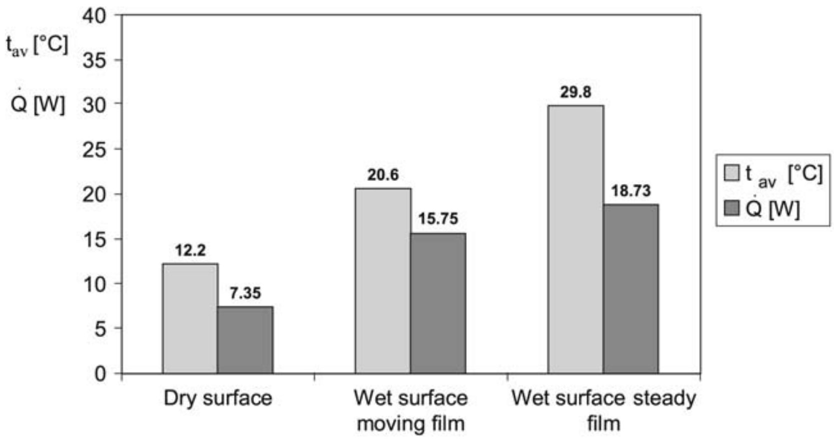

Figure 10.
Transfered heat flux and mean cooled surface temperature

The calculated heat flux is 19 per cent higher than in the case of the moving condensate film. The reason for the lower mean temperature can be found in the additional convective heat transfer in the condensate film, which is a consequence of the film moving.

Conclusions

The paper includes a new approach to the problem of convective-conductive heat and mass transfer between an air flow and a fin surface. In contrast to the available models in the literature, which are mostly one- or two-dimensional, ours is a three-dimensional model.

An advantage of our approach is a more detailed description of the air flow properties and the possibility of calculating the condensate film's thickness with regard to the flow conditions in the film. These factors all have a major influence on local heat transfer. This model avoids having to calculate a heat transfer coefficient, which cannot contain all the local information and the properties of a turbulent flow. In this way, an analysis of heat and mass transfer is possible without empirically calculated quantities.

The influence of the moving condensate film is included in the mathematical model and brings the simulation close to real problem conditions. We have shown that the film flow influences the shape of the film layer and consequently the temperature distribution on the cooled surface.

References

Besednjak, D. and Poredoš, A. (1998), "Efficiency of cooled extended surfaces", *Int. J. Refrigeration*, Vol. 21 No. 5, pp. 372-80.

Chen, L.T. (1991), "Two-dimensional fin efficiency with combined heat and mass transfer between water-wetted fin surface and moving moist air stream", *Int. J. Heat and Fluid Flow*, Vol. 12 No. 1.

Coney, J.E.R., Sheppard, C.G.W. and El-Shafei, E.A.M. (1989), "Fin performance with condensation from humid air: a numerical investigation", *Int. J. Heat and Fluid Flow*, Vol. 10 No. 3.

Kazminejad, H., Yaghoubi, M.A. and Bahri, F. (1993), "Conjugate forced convection-conduction analysis of the performance of a cooling and dehumidifying vertical rectangular fin", *Int. J. Heat Mass Transfer*, Vol. 36 No. 14, pp. 3625-31.

Kilic, A. and Onat, K. (1981), "The optimum shape for convecting rectangular fins when condensation occurs", *Wärme und Stoffübertrangung*, Vol. 15, pp. 125-33.

McQuiston, F.C. (1975), "Fin efficiency with combined heat and mass transfer", *ASHRAE Transactions*, Vol. 81 No. 1, pp. 350-5.

Stephan, K. (1992), *Heat and Mass Transfer in Condensation and Boiling*, Springer Verlag, Berlin.

Tsay, Y.L. (1996), "Effects of binary mixture condensation on turbulent mixed convection heat and mass transfer in a vertical channel", *Numerical Heat Transfer, Part A* No. 29, pp. 599-612.

Wilcox, D.C. (1993), *Turbulence modeling for cfd*, DCW Industries, La Canada.

Wu, G. and Bong, T.Y. (1994), "Overall efficiency of a straight fin with combined heat and mass transfer", *ASHRAE Transaction*, Vol. 100 No. 1, pp. 367-74.